Journal of Power Sources 196 (2011) 9081–9086

Contents lists available at ScienceDirect

Journal of Power Sources

journal homepage: www.elsevier.com/locate/jpowsour

Dynamic behaviour of Li batteries in hydrogen fuel cell power trains

O. Veneri, F. Migliardini, C. Capasso, P. Corbo*

Istituto Motori – National Research Council (CNR), Via Marconi 8, 80125 Naples, Italy

ARTICLE INFO

Article history:
Received 27 October 2010
Received in revised form 14 January 2011
Accepted 5 February 2011
Available online 12 February 2011

Keywords:
PEM fuel cells
Hydrogen
Hybrid vehicles
Lithium battery
Power management

ABSTRACT

A Li ion polymer battery pack for road vehicles (48 V, 20 Ah) was tested by charging/discharging tests at different current values, in order to evaluate its performance in comparison with a conventional Pb acid battery pack. The comparative analysis was also performed integrating the two storage systems in a hydrogen fuel cell power train for moped applications. The propulsion system comprised a fuel cell generator based on a 2.5 kW polymeric electrolyte membrane (PEM) stack, fuelled with compressed hydrogen, an electric drive of 1.8 kW as nominal power, of the same typology of that installed on commercial electric scooters (brushless electric machine and controlled bidirectional inverter). The power train was characterized making use of a test bench able to simulate the vehicle behaviour and road characteristics on driving cycles with different acceleration/deceleration rates and lengths. The power flows between fuel cell system, electric energy storage system and electric drive during the different cycles were analyzed, evidencing the effect of high battery currents on the vehicle driving range. The use of Li batteries in the fuel cell power train, adopting a range extender configuration, determined a hydrogen consumption lower than the correspondent Pb battery/fuel cell hybrid vehicle, with a major flexibility in the power management.

1. Introduction

Current means of transportation are strongly dependent on oil-derived fuels, therefore the possible troubles associated with oil price fluctuations and supply scarcity need to be faced. In addition, their contribution to global anthropogenic emissions of CO_2 is widely recognized. These issues justify the strong interest of research towards new fuels and innovative propulsion systems, in particular different typologies of hybrid electric vehicles present huge potentialities in terms of efficiency and emission control [1]. In this context the hybrid vehicles which adopt an internal combustion engine in addition to an electric drive have already demonstrated their potentiality in having a significant impact on the light duty vehicle market. Furthermore, the hydrogen fuel cell technology has been gaining much attention in recent years as it offers the great advantage to assure the high efficiency and local zero emissions typical of battery powered electric vehicles, improving at the same time their driving range.

In a fuel cell propulsion system the electrochemical generator can be used as the unique power source on board, but the most reliable solutions include the support of electric energy storage systems, such as batteries and/or supercapacitors. Even if the driving range of a fuel cell vehicle depends on the quantity of hydrogen stored on board, the possibility of adopting high performance batteries, such as lithium based systems, is of great interest for range extender hybrid solutions [1,2].

Lithium metal is attractive as battery anode material mainly due to its lightness and high voltage, in spite of some concerns of safety hazard, due to the metal high reactivity. For this reason, in the so-called lithium-ion batteries, both positive and negative electrodes employ lithium "host" compounds, where an intercalation process occurs. In these systems the lithium ion conducting electrolyte is based on a solution of a lithium salt in organic solvents [3], which is not the best solution in terms of safety. Therefore for automotive applications the so-called lithium polymer batteries seem more suitable, since they adopt a solid polymeric electrolyte to transfer lithium ions between the electrodes [4]. The absence of liquid phases facilitates the construction of leak-proof and lightweight containers, which represents an additional advantage for automotive applications.

The most recent developments in this field have been focused on the possibility of reaching very high energy and power densities by using new types of anode, in particular, it has been found that a Si–Li alloy presents a theoretical specific capacity of 4200 mAh g^{-1}, to be compared with 371 mAh g^{-1} of graphite [5,6]. Electrode pulverization phenomena associated with the alloy formation, and the consequent limitation of cycling capability, have led to the research of different solutions, mainly based on reduction of metal particle size down to nanoscale [7,8], utilization of composite materials (in which an inactive component added to the active metal acts as

* Corresponding author. Tel.: +39 081 717 7180; fax: +39 081 239 6097.
E-mail address: p.corbo@im.cnr.it (P. Corbo).

0378-7753/$ – see front matter © 2011 Elsevier B.V. All rights reserved.
doi:10.1016/j.jpowsour.2011.02.012

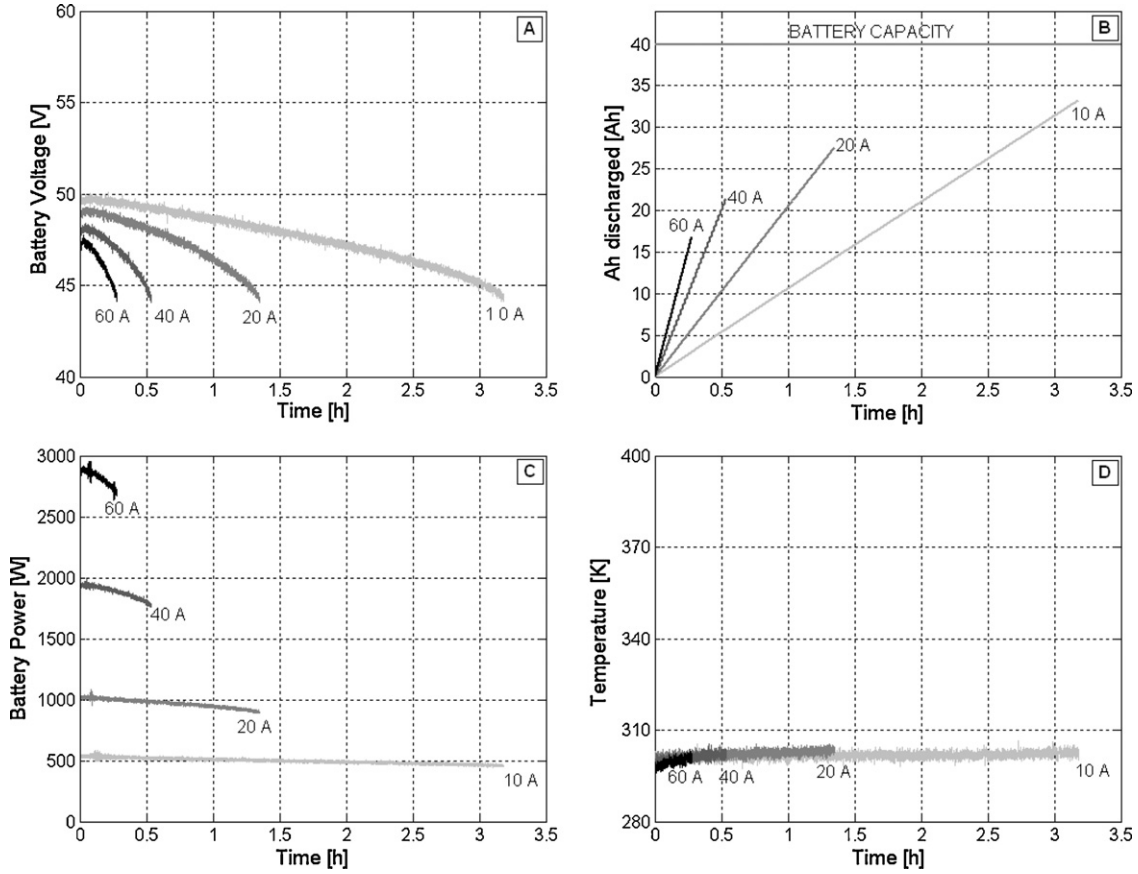

Fig. 1. Discharging test on Pb acid battery pack (48 V, 40 Ah) at different current values. (A) Voltage, (B) Ah discharged, (C) power supplied and (D) battery temperature as function of test length.

a buffer for volume variations) [9,10] or metal hydrides as anode [11]. The researches about the cathode are intensively oriented on high voltage spinels and high capacity layered lithium metal oxides [12–15].

Even with reference to the current technology the lithium polymer batteries represent the state of the art in the field of electric energy storage systems, since they are characterized by very interesting values of the basic electrochemical parameters [5]. Nevertheless storage capabilities able to assure a satisfactory driving range to battery electric vehicles have not yet been reached [16].

The aim of this paper was to compare the behaviour of Li ion polymer with Pb acid battery packs when they supply a hybrid fuel cell power train, working in dynamic conditions representative of actual road load requirements. Both battery packs were characterized in charging/discharging test cycles at different constant current values. The same types of batteries were integrated in a fuel cell power train for moped application, which was installed on a laboratory dynamic test bench. Experimental tests were performed on different load cycles varying acceleration/deceleration rates and duration, in order to obtain indications about fuel economy and dynamic behaviour issues associated with the utilization of those types of batteries in hydrogen fuel cell vehicles.

2. Experimental

The lithium based storage system used in the present work was a lithium ion polymer battery composed by a graphite based anode, a $Li(NiCoMn)O_2$ based cathode and a Li^+ cconducting polymer electrolyte as separator. The battery pack was provided by EiG Battery and its main characteristics and recommended operative conditions are reported in Table 1 in comparison with those of a Pb acid battery pack, provided by Exide Technologies. The lithium and lead battery packs were tested in charging/discharging cycles respecting the recommended values of maximum voltage in charging (54 V for both Li and Pb) and minimum voltage in discharging (39 V for both Li and Pb), in order to avoid battery damages. For these tests the current values for charging and discharging phases were set in the range 4–60 A, compatible with the dynamic conditions required by automotive applications.

The experimental tests with the fuel cell power train were performed using the propulsion system already described in Ref. [17], whose main characteristics are reported in Table 2. It was constituted by fuel cell system (FCS), DC–DC converter, electrical energy storage system, electric drive, and data acquisition systems. The FCS was based on a 2.5 kW PEM stack fuelled with compressed pure hydrogen. The electric drive was based on a LAFERT brushless engine of 1.8 kW nominal power, equipped with a controlled

Table 1
Main characteristics of Pb and Li battery packs.

	Lead battery pack	Lithium battery pack
Nominal voltage	4×12	46.8
Nominal cell voltage	2.0	3.6
Number of cells	6	13
Capacity	40 Ah	20 Ah
Energy	1920 Wh	936 Wh
Specific energy	33 Wh kg^{-1}	105 Wh kg^{-1}
Energy density	99.25 Wh l^{-1}	130 Wh l^{-1}
Operating temperature	−20 +50 °C	−30 +50 °C
Weight	57.6 kg	8.9 kg
Cycle life	500 cycles	1000 cycles
Accessories	–	Auxiliary cooling fan

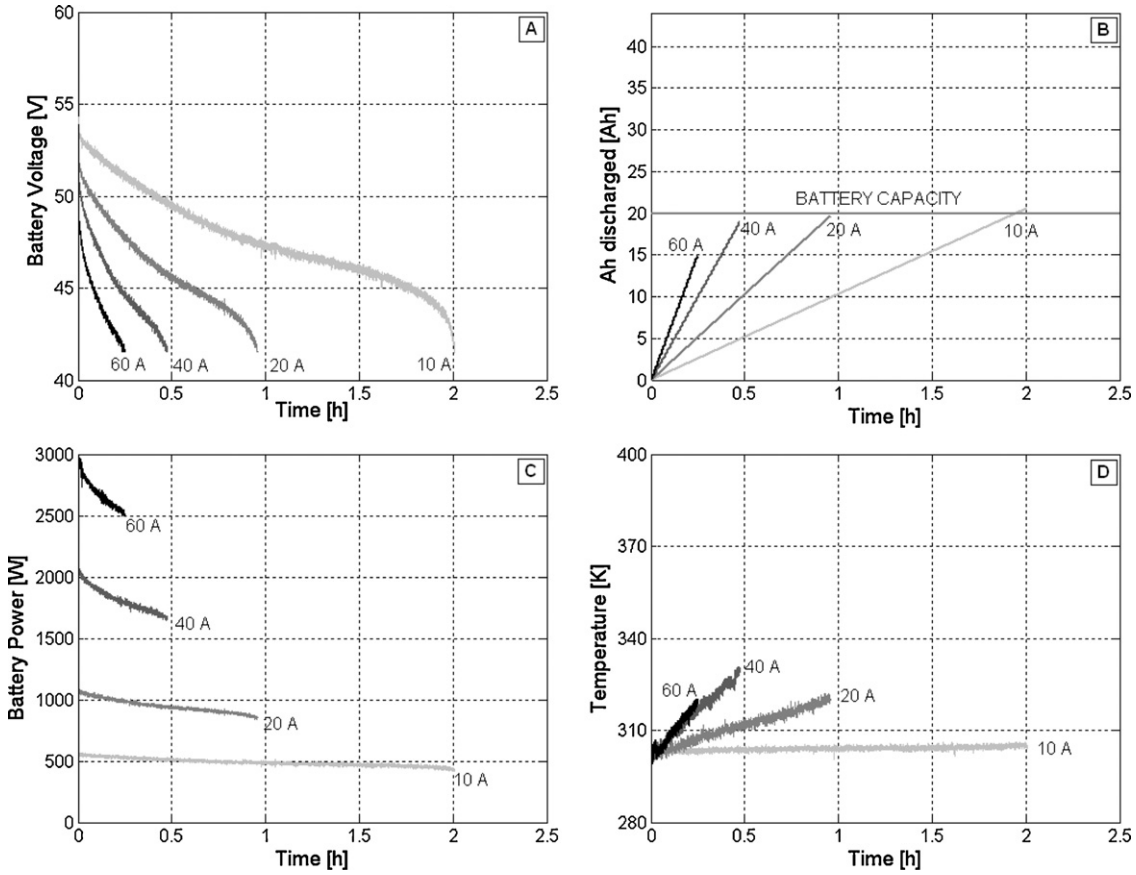

Fig. 2. Discharging test on Li ion polymer battery pack (48 V, 20 Ah) at different current values. (A) Voltage, (B) Ah discharged, (C) power supplied and (D) battery temperature as function of test length.

inverter, whose typology was the same of those installed on electrical commercial scooters. The DC–DC converter, necessary to match the stack output voltage to the values required by the engine, allowed the implementation of control strategies corresponding to different hybrid configurations. The propulsion system was coupled to an electric brake able to perform different driving cycles using a control software specifically developed [17]. The parameters which take into account the vehicle and road characteristics are reported in Table 2.

Table 2
Main characteristics of the fuel cell power train.

Fuel cell system	
FCS electric output	Max 2 kW after DC–DC converter
FCS dynamic	Max change rate 500 W s^{-1}
Hydrogen	Purity of 99.999%Inlet gas pressure: 500 kPa
Air	Side channels compressor 24 VDC, 16 kPa
Water cooling	Circulating pump 24 VDC, 20 kPa, 7 l min^{-1}
Electric drive	
Type	Brushless
Rated power	1.8 kW
Maximum power	2.5 kW
Link voltage	48 V
Rated speed	3000 rpm
Maximum speed	6000 rpm
DC–DC converter	
Inlet voltage range	19–34 V
Rated output voltage	48 V
Rated power	2.8 kW
Vehicle parameters	
Vehicle weight	100 kg (with Li batteries)
Driver weight	80 kg
Vehicle speed	50 km h^{-1} at 6000 rpm

The driving cycles used in tests on the power train were characterized by acceleration and deceleration rates in the range 40–400 W s^{-1}. A control strategy based on a hard hybrid configuration was adopted, setting the power supplied by the fuel cell system at a constant level (600 W). During all the tests the lithium battery packs were air cooled to keep their temperature under the recommended value of 323 K.

3. Results and discussion

The two battery packs described in Section 2 have been firstly characterized by discharging tests at different constant current values. Before these tests, both battery packs were charged at 4 A, corresponding to 0.1 and 0.2 C for Pb and Li battery respectively. The results of these characterizations are reported in Figs. 1 and 2, where voltage, Ah discharged, power supplied and temperature are reported as function of the discharging time. The Pb battery voltage decrease during the discharging phase (Fig. 1A) evidenced the diminution of plate potential, due to the decrease of electrolyte concentration inside plate pores, because of the reduction of diffusion rate inside cells [18]. The test was stopped just before the occurrence of the curve knee, corresponding to an abrupt voltage drop. This phenomenon rapidly increased at higher discharge rates, in particular at 60 A the battery voltage decreased from 48 to 44 V in 0.25 h (Fig. 1A). The effect of this behaviour on the actual battery capacity is shown in Fig. 1B, in terms of Ah discharged versus discharging time. It is evident that the actual capacity of the Pb battery decreased almost linearly with the discharging current, and was always lower than its nominal capacity (40 Ah). In particular resulted 32 Ah at 10 A, and dropped down to 17 Ah at 60 A. The corresponding power values are reported in Fig. 1C, and show a range

from 500 W at the lowest discharging current up to about 3 kW at 60 A, covering the power range required by the engine (Table 2). In Fig. 1D the acquisition of the battery temperature is shown, all values are comprised between 298 and 303 K, evidencing that thermal issues are negligible for Pb batteries.

The discharge curves of Li battery pack are shown in Fig. 2A at the same values of discharging current investigated for Pb batteries. A decrease of battery voltage was observed during the discharge at all current values, evidencing the effect of Li transportation kinetics through the cathode channels and the interface between the solid electrolyte and the electrode [19]. However, differently from Pb batteries, it can be noticed that only at 60 A an appreciable reduction of actual battery capacity was observed, in particular less than 25% of the nominal capacity was lost at 60 A (Fig. 2B). Since voltage range and discharging currents were similar to those adopted in Pb battery tests, also for the Li battery pack the power values resulted compatible with those required by the engine (Fig. 2C), while the thermal behaviour resulted completely different. In Fig. 2D the battery temperature acquisition versus discharging time is shown, evidencing a significant temperature increase starting from 20 A. In particular a temperature of about 328 K was observed at the end of test at 40 A, while a lower temperature was measured at 60 A when the test was stopped at 0.25 h, with a final temperature of about 316 K (the heating rate increased from 1 K h^{-1} at 10 A up to 80 K h^{-1} at 60 A). This aspect could represent a disadvantage of Li batteries when used in an electric vehicle, because it could imply a limitation in power supplying in severe driving conditions (high power requirement for long periods).

The superior performance of Li battery pack resulted evident for all discharging current investigated, and confirmed the suitability of this type of storage system for high dynamic applications, such as those involved in automotive applications. This better performance at high current draw can be attributed to minor transport limitations associated with the higher electrode surface to volume ratio in the Li systems.

In order to confirm the advantages deriving from the utilization of a Li battery pack in an electric propulsion system, some experiments were carried out on the power train without fuel cell generator, performing successive severe load cycles. These were characterized by acceleration of 500 rpm s^{-1}, steady state condition of 100 s at maximum speed (5000 rpm) and torque (2.5 Nm), and deceleration of 250 rpm s^{-1}. These tests were carried out with both Li and Pb batteries in the same vehicle weight condition (Table 2), voltage and current were acquired and the tests were stopped when the minimum voltage tolerated by each battery was reached. The battery state of charge (SOC) was instantaneously calculated during each cycle by the following equation:

$$\mathrm{SOC}(t) = \mathrm{SOC}^{\circ} + \int_{t^{\circ}}^{t} I_{\mathrm{Batt}}(t)\,dt$$

where SOC° is the known battery state of charge at the time t. The comparison between the two battery packs supplying the power train is shown in Figs. 3–5.

During the acceleration phase a maximum current of about 60 A was reached for both systems, whereas during the deceleration phases low negative values of current were reached for a short time due to regenerative braking (Fig. 3). Comparable voltage profiles were also obtained for the two batteries, as they were comprised between the minimum and maximum voltage accepted by both systems (Fig. 4). The difference of duration between the tests, effected with the two batteries, resulted lower than expected on the base of their nominal capacity. In fact the Pb battery pack reached the minimum voltage after about 3000 s, while for Li pack this voltage was reached after 2500 s. The SOC values reported in Fig. 5 clarify this aspect, as 22 out of 40 Ah were discharged from

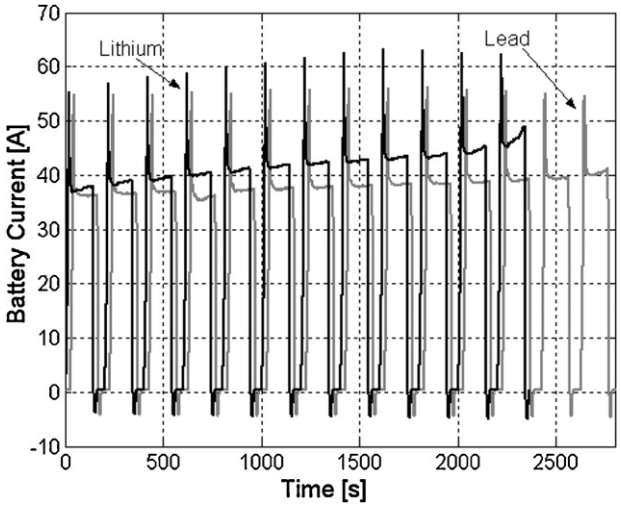

Fig. 3. Battery current acquisition during the complete discharging test on the power train powered by Pb and Li packs.

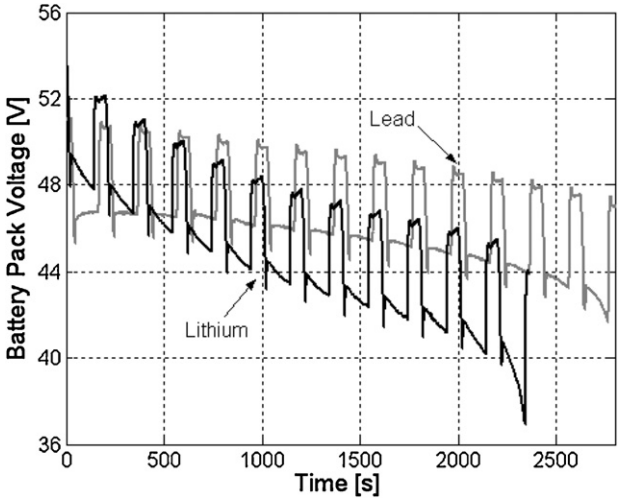

Fig. 4. Battery voltage acquisition during the complete discharging test on the power train powered by Pb and Li packs.

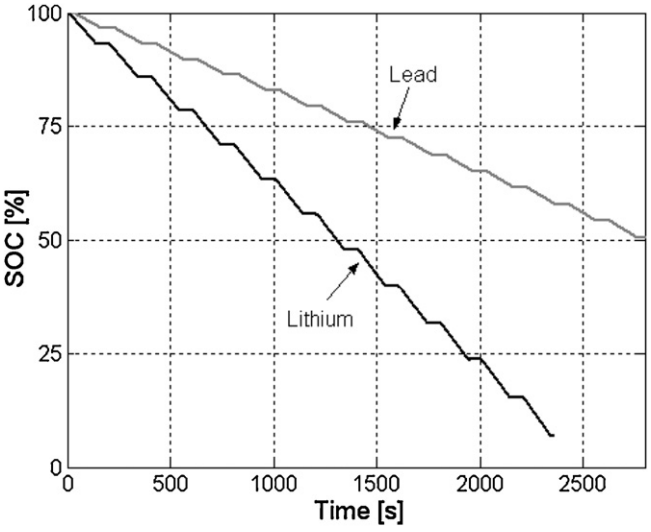

Fig. 5. SOC values during the complete discharging test on the power train powered by Pb and Li packs.

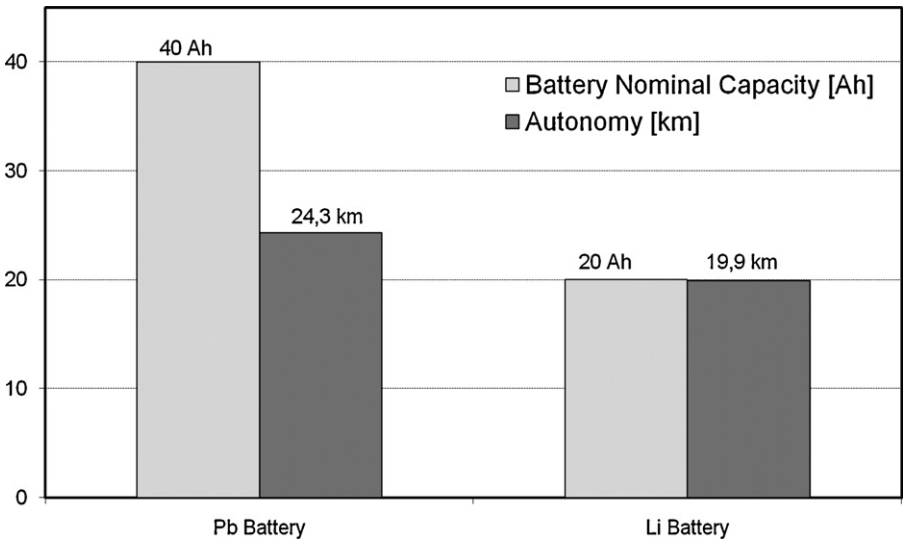

Fig. 6. Comparison between Pb and Li battery packs in terms of driving range in km after the complete discharging test. Nominal capacities are reported for reference.

Pb battery in 3000 s, while almost the total nominal capacity was discharged from Li battery in 2500 s (19 out of 20 Ah). The effect of battery performance on the scooter driving range is shown in the histogram of Fig. 6, in terms of kilometres covered by the vehicle during the tests of Figs. 3–5, together with the nominal capacity of both batteries. It can be noticed that a comparable driving range (20 km for Li, and 24 km for Pb) was covered by the vehicle powered by the two battery packs, in spite of the Li nominal capacity was half of Pb capacity. The different behaviour in terms of driving range between the two battery packs is due to the current profiles of Fig. 3. In fact both battery packs operated during the cycle sequence for the most of time at 40 A, with peaks at 60 A, therefore the discharge was performed in conditions unfavourable for Pb systems (Fig. 1).

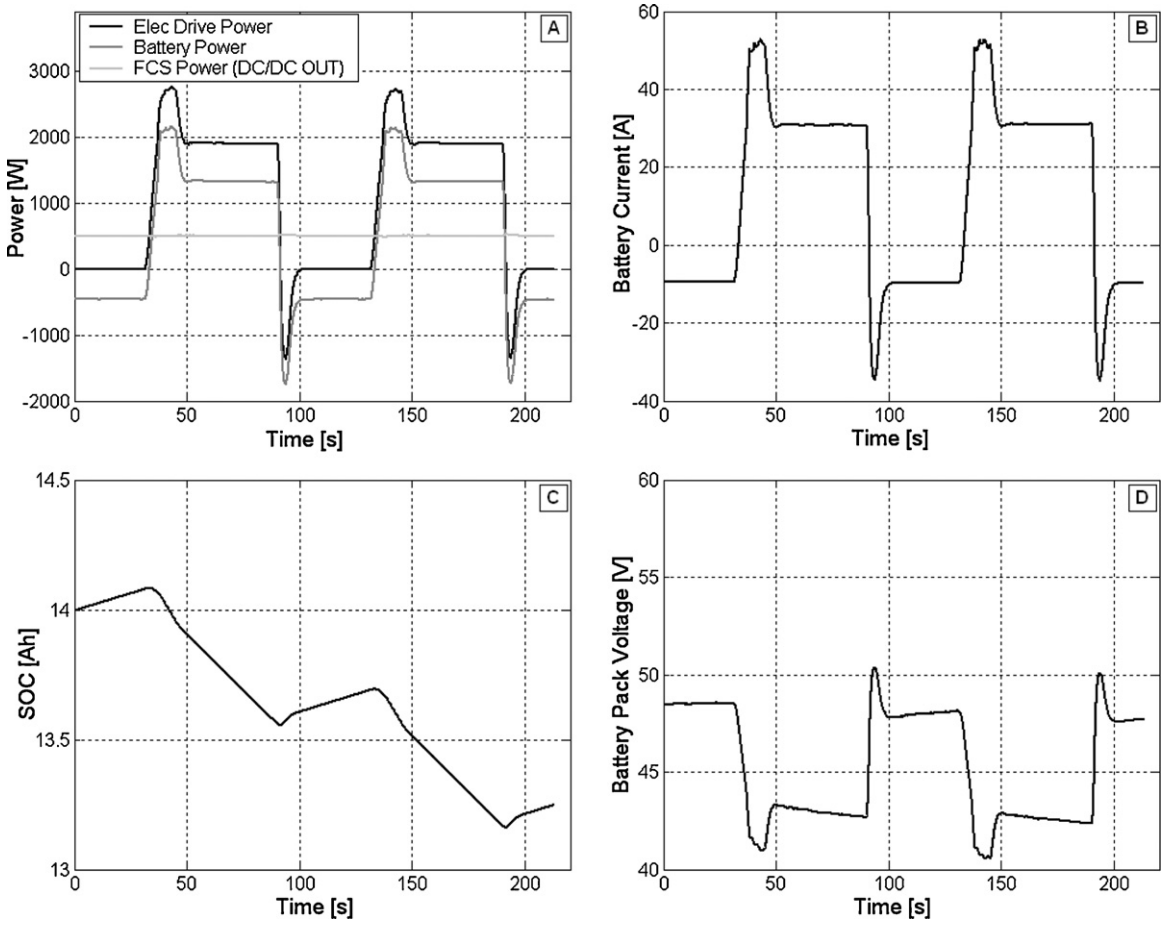

Fig. 7. Fuel cell power train with Li battery pack tested on driving cycle. Acquisition versus time of: (A) power profiles of engine, battery and fuel cell system, (B) battery current, (C) battery voltage, and (D) SOC.

The same power train, integrated with the fuel cell system, was further tested on a series of load cycles characterized by an acceleration phase at 500 rpm s^{-1}, followed by a steady state phase of 50 s and a deceleration at 1000 rpm s^{-1}, while a standstill of 30 s was adopted after each cycle. A range extender hybrid configuration was chosen, in order to fully exploit the dynamic characteristics of the storage system, and utilize the stack in steady state conditions and at a level of generated power much lower than the engine power. The stack power was fixed at 600 W, corresponding to 500 W at the DC–DC converter outlet. In Fig. 7 the results of an experiment conducted on the fuel cell power train with Li battery pack are reported in terms of power profiles, battery current, voltage and SOC versus cycle length. During each cycle the engine power peaked up 2700 W in 10 s, with the steady state phase at 2000 W, while the stationary contribution of the fuel cell system permitted a lower power was delivered from the batteries towards the engine (maximum 2200 W, Fig. 7A). The negative electric power entering the batteries corresponds to both the regenerative braking and battery recharging from the fuel cell system during the standstill phase. The power variations shown in Fig. 7A implied that the battery current ranged for most of the time between 30 and 50 A, during acceleration and steady state phases (Fig. 7B), while negative current peaks of 30 A were detected during the regenerative braking. The SOC profile is reported in Fig. 7C, and evidences the different phases of discharging and recharging of the battery pack, with a decrease of 0.5 Ah during the acceleration and steady state phase, and an increase of 0.1 Ah during regenerative and standstill phase. The battery voltage plot (Fig. 7D) shows that a minimum value of 41 V was reached at the end of the acceleration phase, while in the breaking phase the battery voltage increased from 43 to 50.5 V, remaining within the range of tolerance during the cycle.

Data of Fig. 7 evidence the high dynamic capability of Li batteries, which are able to satisfy the engine requirements during very fast acceleration phases, without appreciable loss of nominal capacity, allowing significant energy recovery during rapid decelerations. The range extender hybrid configuration, with a stack power set at about 25% of the engine maximum power, assured the battery recharging and extended the vehicle driving range. The same test effected with the Pb battery pack, characterized by a nominal capacity twice than Li, showed that identical dynamic performance were obtained by both battery packs utilized in this work.

However, for the cycle shown in Fig. 3 (30–50 A) the Pb storage system, due to the high battery current involved, presented a driving range loss of about 50% with respect to what expected considering its nominal capacity (Fig. 6). Whereas, in the case of the fuel cell vehicle, a higher hydrogen consumption was due to the weight of Pb battery pack, which was about six times higher with respect to Li pack (Table 1) [20]. Consequently, the design of a hybrid fuel cell propulsion system in the range extender configuration could take advantage of the utilization of a Li battery pack, because of the lower weight of the storage system, for the same vehicle mission and power management strategies. On the other hand, the use of high dynamic Li systems at parity of nominal capacity might allow the downsizing of the fuel cell system, as the storage system would provide more power during severe acceleration phases with less capacity losses.

4. Conclusions

Two different battery packs (Li and Pb) have been characterized from the point of view of their application in fuel cell power trains. The experimental results lead to the following conclusions:

- For high discharge currents ($\geq$40 A) the nominal capacity in Ah of Li batteries was almost completely maintained, while the actual capacity of Pb batteries was reduced of about 50%.
- This behaviour had a negative effect on the driving range of the vehicle powered with Pb battery when used in high dynamic driving cycles.
- The tests carried out on a fuel cell power train for scooter application showed that the FC vehicle with Li batteries can offer dynamic performance comparable to that of the FC vehicle equipped with Pb storage systems, but with higher driving range and lower H_2 consumption.
- The use of Li batteries in a FC vehicle, thanks to their better performance on dynamic cycles, might give a major flexibility in the design and energy management of fuel cell power trains, with the possibility of downsizing both storage and FC generation system in the range extender configuration.

References

[1] C.E. Thomas, Int. J. Hydrogen Energy 34 (2009) 6005–6020.
[2] P. Corbo, F. Migliardini, O. Veneri, Renew. Energy 34 (8) (2009) 1955–1961.
[3] Y. Nishi, J. Power Sources 100 (2001) 101–106.
[4] B. Scrosati, F. Croce, S. Panero, J. Power Sources 100 (2001) 93–100.
[5] I. Kuribayashi, M. Yokoyama, M. Yamashita, J. Power Sources 54 (1995) 1–5.
[6] B. Peng, J. Chen, Coord. Chem. Rev. 253 (2009) 2805–2813.
[7] H. Ma, F. Cheng, J.Y. Chen, J.Z. Zhao, C.S. Li, Z.L. Tao, J. Liang, Adv. Mater. 19 (2007) 4067–4070.
[8] C.K. Chan, H. Peng, G. Liu, K. McIlwrath, X.F. Zhang, R.A. Huggins, Y. Cui, Nat. Nanotechnol. 3 (2008) 31–35.
[9] S.H. Ng, J. Wang, D. Wexler, K. Konstantinov, Z.P. Guo, H.K. Liu, Angew. Chem. Int. Ed. 46 (2006) 6896–6899.
[10] J. Hassoun, S. Panero, P. Simon, P.L. Taberna, B. Scrosati, Adv. Mater. 19 (2007) 1632–1635.
[11] Y. Oumellal, A. Rougier, G.A. Nazri, J.M. Tarascon, L. Aymard, Nat. Mater. 7 (2008) 916–921.
[12] J.W. Fergus, J. Power Sources 195 (2010) 939–954.
[13] S. Patoux, L. Daniel, C. Bourbon, H. Lignier, C. Pagano, F. Le Cras, S. Jouanneau, S. Martinet, J. Power Sources 189 (2009) 344–352.
[14] R.K. Katiyar, R. Singhal, K. Asmar, R. Valentin, R.S. Katiyar, J. Power Sources 194 (2009) 526–530.
[15] J. Gao, A. Manthiram, J. Power Sources 191 (2009) 644–647.
[16] G.J. Offer, D. Howey, M. Contestabile, R. Clague, N.P. Brandon, Energy Policy 38 (2010) 24–29.
[17] P. Corbo, F.E. Corcione, F. Migliardini, O. Veneri, J Power Sources 157 (2) (2006) 799–808.
[18] D. Linden, T.B. Reddy, Handbook of Batteries, third edition, McGraw-Hill, New York, 2002, p. 23.36.
[19] H. Kitaura, A. Hayashi, K. Tadanaga, M. Tatsumisago, Electrochim. Acta 55 (28) (2010) 8821–8828.
[20] P. Corbo, F. Migliardini, O. Veneri, J. Power Sources 195 (23) (2010) 7849–7854.